Research Article

Cancer Immunology Research

Role of NOX2-Derived Reactive Oxygen Species in NK Cell–Mediated Control of Murine Melanoma Metastasis

Ebru Aydin[1], Junko Johansson[1], Faisal Hayat Nazir[1,2], Kristoffer Hellstrand[1], and Anna Martner[1]

Abstract

The NADPH oxidase of myeloid cells, NOX2, generates reactive oxygen species (ROS) to eliminate pathogens and malignant cells. NOX2-derived ROS have also been proposed to dampen functions of natural killer (NK) cells and other antineoplastic lymphocytes in the microenvironment of established tumors. The mechanisms by which NOX2 and ROS influence the process of distant metastasis have only been partially explored. Here, we utilized genetically NOX2-deficient mice and pharmacologic inhibition of NOX2 to elucidate the role of NOX2 for the hematogenous metastasis of melanoma cells. After intravenous inoculation of B16F1 or B16F10 cells, lung metastasis formation was reduced in B6.129S6-*Cybb*^{tm1DinK} (*Nox2*-KO) versus *Nox2*-sufficient wild-type (WT) mice. Systemic treatment with the NOX2-inhibitor histamine dihydrochloride (HDC) reduced melanoma metastasis and enhanced the infiltration of IFNγ-producing NK cells into lungs of WT but not of *Nox2*-KO mice. IFNγ-deficient B6.129S7-*Ifng*^{tm1Ts}/J mice were prone to develop melanoma metastases and did not respond to *in vivo* treatment with HDC. We propose that NOX2-derived ROS facilitate metastasis of melanoma cells by downmodulating NK-cell function and that inhibition of NOX2 may restore IFNγ-dependent, NK cell–mediated clearance of melanoma cells. *Cancer Immunol Res; 5(9); 804–11. ©2017 AACR.*

Introduction

Reactive oxygen species (ROS) are short-lived compounds that arise from electron transfer across biological membranes where the electron acceptor is molecular oxygen and the initial product is superoxide anion (O_2^-). ROS refer to oxygen radicals such as O_2^- and the hydroxyl radical ($OH^·$) along with nonradicals, including hydrogen peroxide, that share the oxidizing capacity of oxygen radicals and may be converted into radicals (1). ROS are generated as by-products of mitochondrial ATP generation in the electron transport chain but are also produced in a regulated fashion by the NADPH oxidases (NOX) and the dual oxidases (DUOX). This family of transmembrane proteins comprises NOX1-5 and DUOX1-2, whose only known function is to produce ROS (2).

The NOX proteins are structurally similar and utilize a similar principal mechanism of ROS generation but vary in cellular and subcellular distribution. NOX2 is expressed almost exclusively in cells of the myeloid lineage such as monocyte/macrophages and neutrophilic granulocytes (3, 4). These cells utilize NOX2-derived ROS to eliminate intra- and extracellular microorganisms (5). NOX2 has also been linked to immunosuppression in cancer: when released from myeloid cells into the extracellular space, ROS generated by NOX2 may trigger dysfunction and apoptosis of adjacent antineoplastic lymphocytes, including natural killer (NK) cells (6–9). The strategy to target ROS formation by myeloid cells has been proposed to improve the efficiency of cancer immunotherapy (3, 10–12).

The role of ROS and NOX2 for the growth and metastatic spread of cancer cells is, however, complex and controversial. Thus, although the genetic disruption of *Nox2* reduces the subcutaneous growth of murine melanoma and lung carcinoma, it does not affect sarcoma growth or prostate cancer growth in mice (13, 14). Also, the *in vivo* administration of scavengers of ROS such as *N*-acetyl-cysteine reduces the tumorigenicity of murine melanoma cells (15) but enhances lymph node metastasis in other melanoma models, accelerates tumor progression in mouse models of B-RAF- and K-RAS-induced lung cancer and accelerates the metastasis of xenografted human melanoma cells in immunodeficient mice (16–18).

The detailed mechanisms of relevance to the discrepant impact of ROS for the growth and spread of cancer cells remain to be elucidated. Further understanding of the role of ROS for cancer progression requires experimental models that address a distinct phase of tumor progression, define the source of ROS, and take mechanisms of immunosurveillance into account. For the present study, we aimed at determining the impact of genetic and pharmacologic inhibition of NOX2 in a murine NK cell–dependent model of melanoma metastasis.

Materials and Methods

Culture of cell lines

B16F1 and B16F10 murine melanoma cells were obtained in 2013 from the Cell Culture Laboratory at the Department of Virology, University of Gothenburg, where cells were

[1]TIMM Laboratory, Sahlgrenska Cancer Center, University of Gothenburg, Gothenburg, Sweden. [2]Department of Psychiatry and Neurochemistry, University of Gothenburg, Gothenburg, Sweden.

Corresponding Author: Anna Martner, University of Gothenburg, Medicinaregatan 1F, 40530 Gothenburg, Sweden. Phone: 46-736-517644; Fax: 46-31-84-61-13; E-mail: anna.martner@gu.se

doi: 10.1158/2326-6066.CIR-16-0382

authenticated by melanotic morphology and checked for absence of mycoplasma using PCR before freezing aliquots. Each aliquot was thawed and cultured for no more than 1 week for each experiment. Cells were cultured in Iscoves' medium containing 10% FCS (Sigma-Aldrich), 2 mmol/L L-glutamine, 1 mmol/L sodium pyruvate, 100 U/mL penicillin, and 100 mg/mL streptomycin at 37°C, 5% CO_2 for 1 week before inoculation into mice.

Induction of lung metastasis in *Nox2*-KO and *Ifng*-KO mice

All animal experiments were approved by the Research Animal Ethics Committee in Gothenburg. Mice were maintained under pathogen-free conditions according to guidelines issued by the University of Gothenburg. C57BL/6 mice were obtained from The Charles River Laboratories. B6.129S6-*Cybb*^{tm1Din}(*Nox2*$^{-/-}$ or *Nox2*-KO) mice that lack the myeloid gp91^{phox} subunit NOX2 and, thus, a functional ROS-forming NOX2 were obtained from The Jackson Laboratory. B6.129S7-*Ifng*^{tm1Ts}/J (*Ifng*$^{-/-}$ or *Ifng*-KO) mice that do not produce IFNγ (19) were kindly provided by Prof. Nils Lycke, MIVAC at University of Gothenburg. Naïve C57BL/6, *Nox2*-KO, and *Ifng*-KO mice (6—12 weeks of age) were treated intraperitoneally (i.p.) with PBS (control), HDC (Sigma, 1,500 μg/mouse), IL15 (0.04 μg/mouse), alone or combined, on the day before, the day after, and 3 days after intravenous (i.v.) inoculation of B16F10 cells (5×10^4–15×10^4 cells/mouse) or B16F1 cells (20×10^4–30×10^4 cells/mouse). Three weeks after tumor inoculation, mice were euthanized by cervical dislocation followed by harvesting of lungs and spleens. Lung metastasis was determined by counting visible pulmonary metastatic foci under a light microscope. The experimental design is outlined in Fig. 1A.

For assessment of the impact of NOX2 inhibition on immune parameters during the early phase of tumor progression, mice received HDC at 1,500 μg/mouse or PBS (control) 1 day before the inoculation of B16F10 cells followed by dissection of lungs at 30 minutes or 24 hours after tumor cell inoculation as shown in Fig. 2A. In the latter experiments, naïve mice and HDC-treated mice that did not receive melanoma cells were used as additional controls.

Preparation of single-cell suspensions from lungs and spleens

Lung tissues were dissociated into single cells by combining enzymatic degradation of extracellular matrix with mechanical dissociation using gentle MACS Technology (Miltenyi Biotech) based on instructions provided by the manufacturer. Single-cell suspensions of splenocytes were prepared by mashing the spleens through a 70-μm cell strainer followed by depletion of erythrocytes using RBC Lysing buffer (Sigma-Aldrich).

Flow cytometry

The following fluorochrome-labeled antimouse mAbs were purchased from BD Biosciences: anti-CD45 (30-F11), anti-CD11c (HL3), anti-IaIe (2G9), anti-CD3 (145-2311), anti-CD4 (RM4-5), anti-CD8 (53-6.7), anti-NK1.1 (PK136), anti-CD19 (1D3), anti-CD11b (M1/70), anti-Gr1 (RB6-8C5), anti-CD40 (3/23), and anti-Ly6C (AL-21). Anti-CD33 (29A1.4) was from Ebiosciences; anti-F4/80 (BM8) and anti-CD69 (H1.2F3) were from BioLegend. LIVE/DEAD Fixable Yellow Dead Cell Stain Kit or DAPI (both from Invitrogen) were used as cell viability markers in flow cytometry analyses. A minimum of 100,000 gated live cells were collected on a four-laser BD LSRFortessa (405, 488, 532, and 640 nm). Data were analyzed using FACSDiva Version 8.0.1 software (BD Biosciences).

Detection of ROS

Superoxide anion production was determined by use of the isoluminol-electrogenerated chemiluminescence technique as described elsewhere (20). Briefly, single-cell suspensions of lungs were diluted to 10^7 cells/mL in Krebs-Ringer glucose buffer supplemented with isoluminol (10 mg/mL; Sigma-Aldrich) and horseradish peroxidase (HRP, 4 U/mL, Boehringer) and added to 96-well plates that were incubated at 37°C. Phorbol myristate acetate (PMA, 5×10^{-8} M, Sigma-Aldrich) or the formyl peptide receptor agonist WKYMVm (10^{-5} M, Tocris Bioscience) were added for induction of ROS production. Light emission was recorded continuously using a FLUOstar Omega plate reader (BMG). In some experiments, HDC (10–1,000 μmol/L, final concentrations) was added 5 minutes prior to the addition of WKYMVm.

Depletion of Gr1$^+$ and NK cells *in vivo*

Gr1$^+$ cells were depleted by i.p. injections of 400 μg anti-Gr1 antibody (BioXCell, Clone RB6-8C5) 2 days before B16 cell inoculation. This procedure depletes >95% of Gr1$^+$ cells in blood and other tissues (21). NK cells were depleted by i.p. injections of 250 μg anti-NK1.1 antibody (BioXCell, Clone PK136) 4 days and 2 days before B16F10 cell inoculation. NK-cell depletion was confirmed by flow cytometry on lungs and spleen tissue harvested on days 1, 3, and 6 after antibody injection.

NK-cell isolation and adoptive transfer

Spleens were harvested from WT C57BL/6 mice and single-cell suspensions were prepared. Splenocytes were enriched for NK cells by passage through nylon wool columns (Polysciences). NK cells were then negatively selected using an NK-cell isolation kit II (Miltenyi Biotech) according to the manufacturer's instructions to a purity of >70%. Five million enriched NK cells were injected i.v. 12 hours before inoculation of B16F10 cells. WT NK cells in *Ifng*$^{-/-}$ mice were detected 2 days after adoptive transfer by collecting peripheral blood followed by DNA extraction and PCR. The primer pair used for detection of WT *Ifng* was 5′AGAAGTAAGTGGAAGGGCCCAGAAG 3′ and 5′AGGGAAACTGGGAGA GGAGAAATAT 3′. For detection of the disrupted IFNγ gene (*Ifng*$^{-/-}$) the primer pair 5′TCAGCGCAGGGGCGCCCGGTTCTTT 3′ and 5′ ATCGACAAGACCGGCTTCCATCCGA 3′ was used (19).

Detection of IFNγ

Mice were pretreated with HDC (1,500 μg) or PBS on the day before i.v. inoculation of B16F10 cells. Thirty minutes after tumor cell inoculation mice were sacrificed and single-cell lung cell suspensions were prepared. Lung cells were cocultured overnight with B16 cells (500,000 cells/mL) in flat bottom 96-well plates at effector:target cell ratios of 1:1 to 50:1. Supernatants were collected after 24 hours and the IFNγ content was determined by ELISA (Mouse IFNγ DuoSet ELISA, R&D Systems).

Statistical analysis

Two-tailed paired or unpaired *t* tests were used for statistical calculations. For multiple comparisons, one-way ANOVA followed by the Holm–Sidak multiple-comparison test was used.

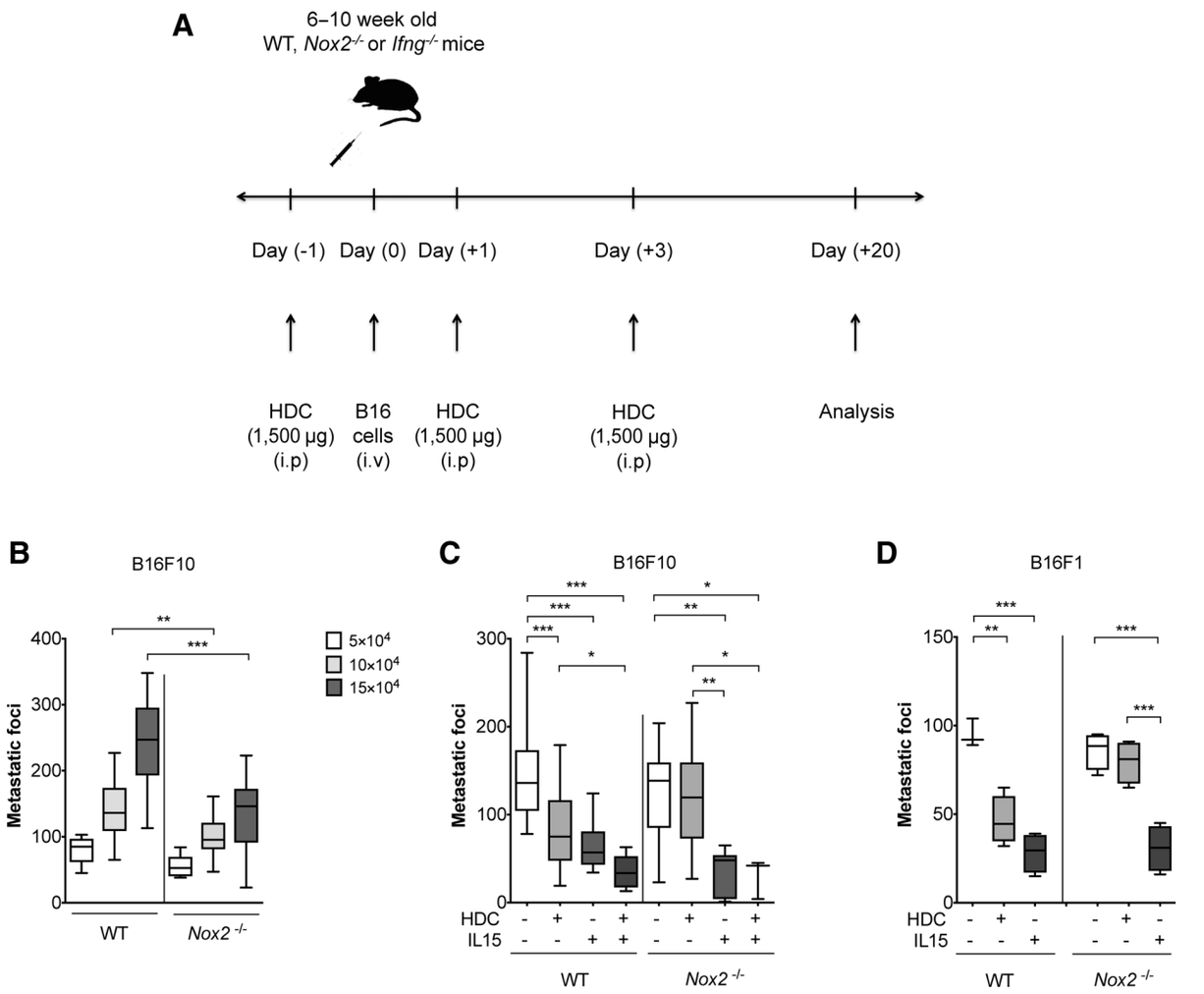

Figure 1.

Impact of genetic and pharmacologic inhibition of NOX2 on B16 melanoma metastasis. **A,** The experimental design. **B,** The number of metastatic foci formed in lungs of WT and *Nox2*-KO (*Nox2*$^{-/-}$) mice at 3 weeks after i.v. inoculation of 50,000, 100,000, or 150,000 B16F10 cells. Medians and quartiles are indicated by boxes. Error bars show the min to max values ($n = 6$ for each group; *t* test; two independent experiments). **C**, The number of metastatic foci in lungs of WT or *Nox2*-KO mice after systemic treatment with HDC and/or IL15. In these experiments, 100,000 B16F10 cells were injected into WT mice and 150,000 cells into *Nox2*$^{-/-}$ mice to achieve comparable levels of baseline metastasis ($n = 15$ for all groups of WT mice; $n = 8$ for control, HDC and IL15 groups of *Nox2*$^{-/-}$ mice and $n = 3$ for HDC + IL15). Combined treatment with IL15 and HDC was significantly more effective than IL15 alone to reduce metastasis formation in WT mice, when analyzed by *t* test, $P = 0.01$ (up to five independent experiments). **D**, Results from lung metastasis formation by the B16F1 melanoma cell line. This cell line is less metastatic compared with B16F10 and, therefore, 200,000 B16F1 cells were injected into WT mice and 300,000 cells into *Nox2*$^{-/-}$ mice. The number of metastatic foci in lungs of WT and *Nox2*-KO mice after systemic treatment with HDC or IL15 was determined after 3 weeks. ($n = 4$ for all groups except $n = 3$ for control group of WT mice). The results shown in Fig. 1C–D were evaluated by repeated measures ANOVA. Nonsignificant values: n.s., $P > 0.05$; *, $P \leq 0.05$; **, $P \leq 0.01$; ***, $P \leq 0.001$.

Results

Inhibition of NOX2 reduces hematogenous melanoma metastasis

To elucidate the role of NOX2-derived ROS in murine melanoma metastasis, we utilized genetically modified mice that lack the myeloid gp91^{phox} subunit NOX2 and thus a functional ROS-producing NOX2 in myeloid cells (*Nox2*-KO mice). Over a range of amounts of i.v. inoculated B16F10 cells, it was observed that the establishment of melanoma metastases was less pronounced in lungs of *Nox2*-KO mice compared with WT B6 mice (Fig. 1B). We next evaluated effects of HDC, a NOX2-inhibitor (22), on melanoma metastasis in WT and *Nox2*-KO mice. These experiments were performed using loads of injected B16F10 cells that produced comparable numbers of metastases in WT and *Nox2*-KO animals; that is, 100,000 B16F10 cells for WT mice and 150,000 cells for *Nox2*-KO mice. In agreement with a previous report (23), systemic treatment of mice with HDC (1,500 µg/mouse i.p.) during the initial phase of melanoma engraftment (days −1, 1, and 3 after tumor cell inoculation) decreased the number of lung metastases in WT mice. These effects were not observed in *Nox2*-KO mice (Fig. 1C). The NK cell-activating cytokine IL15 (24; 0.04 µg/mouse on days −1, 1, and 3) exerted antimetastatic activity *in vivo* in WT and *Nox2*-KO mice (Fig. 1C). Combined treatment with

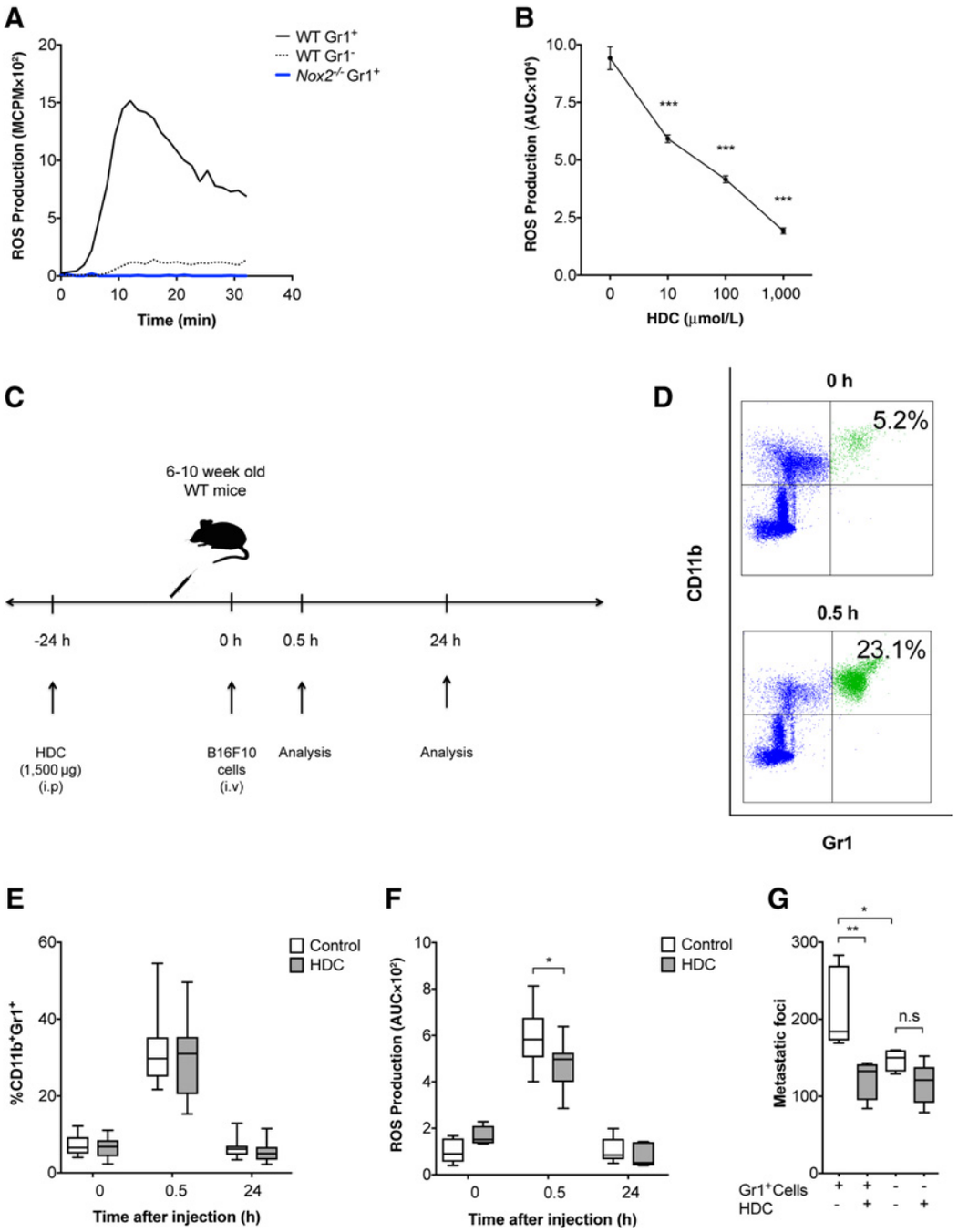

Figure 2.

Effect of HDC on the ROS production in mouse lungs after melanoma cell inoculation. **A**, The extracellular ROS production of PMA-stimulated WT $Gr1^+$ (black solid line), WT $Gr1^-$ (black dashed line), or $Nox2^{-/-}$ $Gr1^+$ mouse lung cells (blue line) in a representative experiment out of three performed. **B**, The ROS production of WT lung cells triggered by 10^{-7} M WKYMVm in response to HDC at indicated final concentrations. The mean ROS production ± SEM is displayed ($n = 3$, t test). **C,** The experimental design designed to assess the dynamics of ROS-producing myeloid cells in lungs after B16 cell inoculation. **D**, A representative dot plot of $CD11b^+Gr1^+$ cells out of live $CD45^+$ lung cells before (0 hour) or 0.5 hours after tumor cell inoculation. **E**, The fraction of $CD11b^+Gr1^+$ cells out of live $CD45^+$ cells in lungs at indicated time points after tumor cell injection, with or without pretreatment of mice with PBS (control) or HDC 24 hours before analysis, as determined in single-cell lung suspensions ($n = 18$ in each group; four independent experiments). **F**, The ROS formation (area under curve, AUC) *ex vivo* in response to PMA stimulation of single lung cell suspensions from mice pretreated with HDC or PBS on the day before tumor cell inoculation. ROS production was determined at 30 minutes and 24 hours after inoculation of 100,000 B16 cells ($n = 5$–10, t test; three independent experiments). **G**, A reduced B16F10 metastasis formation and lack of effects of systemic treatment with HDC on metastasis formation in animals depleted of $Gr1^+$ cells prior to melanoma cell inoculation ($n = 4$–5 for each group, one way ANOVA). Nonsignificant values: n.s., $P > 0.05$; *, $P \leq 0.05$; **, $P \leq 0.01$; ***, $P \leq 0.001$.

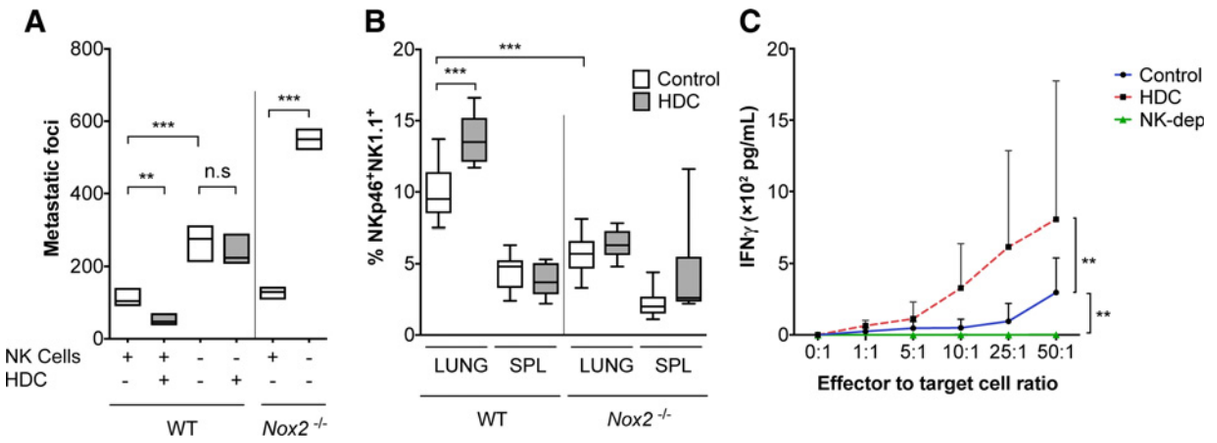

Figure 3.

Antimetastatic effects of HDC rely on NK cells and NK cell–derived IFNγ. **A**, The effects of systemic treatment with HDC on B16F10 metastasis formation in WT and *Nox2*$^{-/-}$ animals depleted of NK cells ($n = 7$ for untreated WT mice with and without NK cells (two independent experiments); $n = 3$ for HDC-treated WT mice with and without NK cells; $n = 4$ for each group of *Nox2*$^{-/-}$ mice, one way ANOVA). **B**, Effects of systemic treatment with HDC on NK-cell numbers in lungs and spleens of WT and *Nox*-KO (*Nox2*$^{-/-}$) mice at 3 weeks after tumor cell inoculation. The percentage of NK cells out of live CD45$^+$ cells was determined by flow cytometry (WT mice $n = 9$–11; *Nox2*$^{-/-}$ mice $n = 9$–13, *t* test; three independent experiments). **C**, IFNγ levels produced in lung cells from HDC-treated and control WT mice that were incubated with B16 melanoma cells at indicated effector to target cell ratios. Mice received HDC or PBS (control) 24 hours before i.v. inoculation of B16 cells. Lungs were recovered 30 minutes after tumor cell inoculation ($n = 11$ for the control group, $n = 6$ for the other groups, two-way ANOVA; two independent experiments). Nonsignificant values: n.s., $P > 0.05$; *, $P \leq 0.05$; **, $P \leq 0.01$; ***, $P \leq 0.001$.

HDC and IL15 additively reduced B16F10 metastasis in WT mice but not in *Nox2-KO* mice (Fig. 1C). Experiments using the B16F1 strain of melanoma cells (25) confirmed the reduced level of metastasis in *Nox2*-KO mice and the NOX2-dependent, antimetastatic effect of HDC *in vivo* (Fig. 1D).

HDC targets ROS formation *in vitro* and *in vivo*

CD11b$^+$Gr1$^+$ myeloid cells express NOX2 and constitute the principal source of extracellular ROS in blood and tissue (26, 27). Accordingly, CD11b$^+$Gr1$^+$ cells isolated from the lungs of naïve WT mice, but not from *Nox2*-KO mice, produced extracellular ROS upon stimulation, whereas the Gr1$^-$ fraction of lung cells produced minute extracellular ROS (Fig. 2A). ROS formation from WT lung cells was dose-dependently suppressed by HDC *in vitro* (Fig. 2B).

In experiments designed to assess the dynamics of ROS-producing myeloid cells in lungs after B16F10 cell inoculation (Fig. 2C), we observed a pronounced and transient influx of CD11b$^+$Gr1$^+$ myeloid cells into lungs at 30 minutes after i.v. inoculation of tumor cells (Fig. 2D and E). Systemic treatment with HDC prior to melanoma cell inoculation did not alter the degree of influx of myeloid cells into lungs (Fig. 2E) but reduced the ROS formed *ex vivo* in lung cell suspensions (Fig. 2F). To further clarify the impact of CD11b$^+$Gr1$^+$ cells on melanoma metastasis, Gr1$^+$ cells were depleted from WT mice before treatment of mice with HDC and i.v. inoculation of B16F10 cells. The extent of lung metastasis was reduced in the absence of Gr1$^+$ cells. Systemic treatment with HDC did not affect metastasis in Gr1$^+$-depleted mice (Fig. 2G).

Role of NK cells for melanoma metastasis in WT and *Nox2*-KO mice

NK-cell function is reportedly critical to limit lung metastasis in experimental models of murine melanoma (23, 28). To define the role of NK cells in the context of NOX2 inhibition, WT and *Nox2*-KO mice were depleted of NK cells by anti-NK1.1 antibody treatment prior to melanoma cell inoculation. NK-cell depletion more than doubled metastasis formation in WT and *Nox2*-KO mice. HDC did not inhibit melanoma metastasis in animals depleted of NK cells (Fig. 3A). In experiments designed to clarify whether the reduced ROS levels in lungs following administration of HDC translated into altered NK-cell function at the site of tumor expansion, it was observed that treatment of mice with HDC entailed increased NK-cell counts in lungs, but not in spleen, at 3 weeks after tumor cell inoculation (Fig. 3B). Unexpectedly, we detected fewer NK cells in lungs and spleens of *Nox2*-KO mice than in WT animals (Fig. 3B). Also, as shown in Fig. 3A, the degree of metastasis was strikingly enhanced in NK cell–depleted *Nox2*-KO mice, which may point toward the possibility of increased functionality of NK cells in the absence of NOX2.

NOX2 inhibition enhances the capacity of lung NK cells to produce IFNγ

As the antimetastatic functions of NK cells in the B16 model reportedly rely on the formation of IFNγ (29, 30), we assessed the IFNγ production of pulmonary NK cells from *Nox2*-KO and WT mice. Lung cells were isolated 30 minutes after B16F10 cell inoculation and IFNγ production was then assessed upon coculture of lung cells with B16F10 cells *in vitro*. Only minor amounts of IFNγ (<25 pg/mL) were detected when lung cells or B16 cells were cultured alone. Also, minute levels (<10 pg/mL) of IFNγ were produced in cocultures of lung cells and B16 cells after the depletion of NK cells *in vivo* using anti-NK1.1, thus supporting that the IFNγ produced in these cell cultures was contributed by NK cells (Fig. 3C). It was further observed that lung NK cells from *Nox2*-KO mice produced significantly higher amount of IFNγ *ex vivo* at a lung cell to melanoma cell ratio of 50:1 compared with lung NK cells from WT mice (WT vs. *Nox2*-KO lungs; 297 ± 81 vs. 749 ± 27 pg/mL, respectively; $P = 0.004$, *t* test). A similar experimental design was adopted to assess the impact of

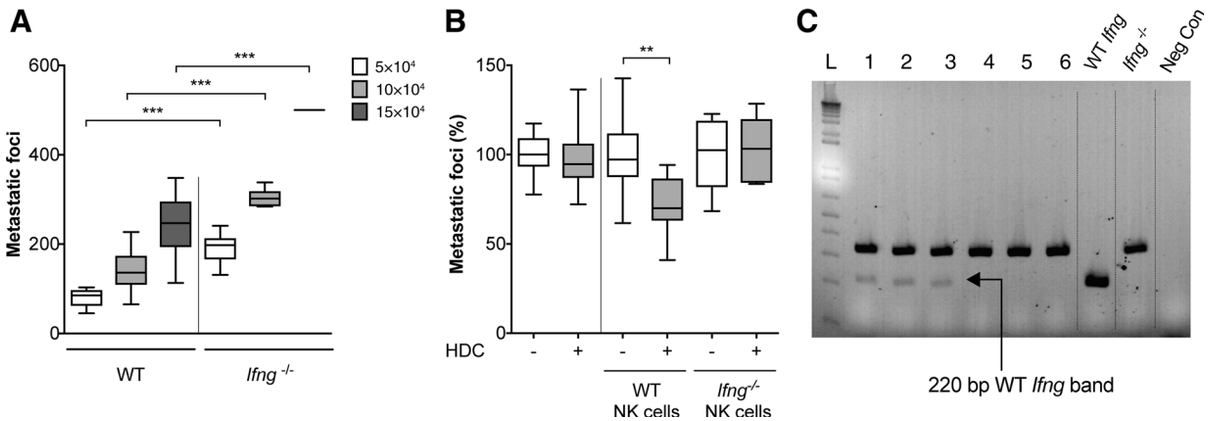

Figure 4.

Impact of IFNγ in B16 melanoma metastasis. **A**, Box plots of B16F10 metastasis at 3 weeks after i.v. inoculation of 50,000, 100,000, or 150,000 B16 melanoma cells into WT and *Ifng*$^{-/-}$ mice ($n = 6$ for each group, *t* test; two independent experiments). **B**, Left, the lack of efficacy of systemic treatment with HDC on metastasis formation at 3 weeks after inoculation of B16 melanoma cells into *Ifng*$^{-/-}$ mice ($n = 19$–21, *t* test; four independent experiments). **B**, Right, effects of systemic treatment with HDC on metastasis formation (% of control) in *Ifng*$^{-/-}$ mice that received the adoptive transfer of purified NK cells from WT mice ($n = 9$ for each group, *t* test) or purified NK cells from *Ifng*$^{-/-}$ mice ($n = 6$, *t* test; two independent experiments). **C**, The presence of WT *Ifng* in peripheral blood collected from six representative *Ifng*$^{-/-}$ mice who had received adoptive transfer of WT NK cells (lanes 1–3) or *Ifng*$^{-/-}$ NK cells (lanes 4–6) 2 days earlier. PCR was performed for WT *Ifng* and the disrupted IFNγ gene of *Ifng*$^{-/-}$ mice. Nonsignificant values: n.s., $P > 0.05$; *, $P \leq 0.05$; **, $P \leq 0.01$; ***, $P \leq 0.001$.

pharmacologic NOX2 inhibition by HDC on the formation of IFNγ in lungs. Lung cells were isolated from HDC-treated or control WT mice at 30 minutes after B16F10 cell inoculation. When lung cells were cocultured with the B16 cells, higher concentrations of IFNγ were produced *ex vivo* by lung NK cells isolated from mice treated with HDC *in vivo* (Fig. 3C).

Role of IFNγ in NOX2-mediated control of melanoma metastasis

We next assessed the capacity of B16F10 cells to form metastases in *Ifng*-KO versus WT mice. In accordance with earlier studies (29, 30), melanoma metastasis was enhanced in IFNγ-deficient mice (Fig. 4A). Systemic treatment with HDC did not reduce melanoma metastasis in *Ifng*-KO mice (Fig. 4B). The adoptive transfer of IFNγ-producing WT NK cells, but not the transfer of *Ifng*-KO NK cells, to *Ifng*-KO mice significantly restored the antimetastatic efficacy of HDC (Fig. 4B). Presence of cells with *Ifng*$^{+/+}$ genotype in blood of *Ifng*-KO mice was confirmed by PCR at 2 days after the adoptive transfer of WT NK cells (Fig. 4C).

Discussion

We report that genetic inhibition of NOX2, which mediates oxidative stress by generating ROS from myeloid cells, reduced the capacity of two strains of murine melanoma cells (B16F1 and B16F10) to form lung metastases after i.v. inoculation, apparently by facilitating NK cell–mediated clearance of malignant cells. Also, treatment of mice with the NOX2 inhibitor HDC reduced melanoma metastasis in WT but not in *Nox2*-KO mice. Our results concur with a study showing that HDC reduces the subcutaneous growth of EL-4 thymoma tumors in WT but not in *Nox2*-KO mice (31), thus, underscoring that the antineoplastic efficacy of HDC depends on the availability of NOX2.

Our results also show that the establishment of melanoma metastases was associated with a rapid and transient accumulation of ROS-forming CD11b^{+}Gr1^{+} myeloid cells in the lung parenchyma and that the ROS-forming capacity of infiltrating myeloid cells *ex vivo* was suppressed by the *in vivo* administration of HDC. Pharmacologic inhibition of NOX2 also entailed increased numbers of lung NK cells in tumor-bearing mice. In agreement with earlier studies (29, 30), the availability of IFNγ was critical for NK cell–mediated clearance of B16 melanoma cells from lungs. Furthermore, the antimetastatic effect of HDC was absent in *Ifng*-KO mice but could be reconstituted by the adoptive transfer of *Ifng*$^{+/+}$ NK cells. Collectively, these results imply that the antimetastatic properties of HDC rely on the availability of NK cell-derived IFNγ. We observed that despite the more efficient NK cell–mediated clearance of melanoma cells in *Nox2*-KO, rather than in WT mice, higher counts of NK cells were detected in the lung parenchyma of WT mice. This finding implies that NK cells were more efficient effector cells on a per cell basis in *Nox2*-KO mice. In agreement with this hypothesis, we observed that pulmonary NK cells from *Nox2*-KO mice showed enhanced formation of IFNγ *ex vivo*.

From these results, we hypothesize that NOX2-derived ROS produced by myeloid cells may exert oxidative stress with ensuing reduction of NK cell–mediated clearance of melanoma cells and aggravation of metastasis. In agreement with our findings, the subcutaneous growth of murine melanoma and lung carcinoma was reduced in *Nox2*-KO mice (13). However, several studies report contradictory effects of ROS on the course of experimental melanoma and other forms of cancer, in particular regarding direct effects of ROS on tumor cells. Cancer cells, thus, display elevated ROS concentrations due to enhanced metabolism and mutations that trigger oxidative processes (32–34). The increased ROS may promote mutagenesis and may also render tumor cells more prone to expand and produce distant metastases (34–37). In agreement, overexpression of the antioxidant SOD3 inhibits murine breast cancer cell metastasis (38), and the ROS scavenger *N*-acetyl-cysteine reduces the tumorigenicity of murine melanoma cells (15).

High endogenous ROS concentrations in malignant cells may also render these cells more vulnerable to further stresses (34, 39, 40). Hence, anticancer therapies that trigger a further increase in ROS formation may induce cell death in cancer cells compared with their non-malignant counterparts (34, 41, 42). In addition, ROS can limit malignant growth by triggering activation of p53, whereas antioxidants enhanced tumor progression in a p53-dependent manner (17). Antioxidants can enhance lymph node metastasis in a model of genetically related melanoma (16). In immunodeficient NOD-SCID-*Il2rg*$^{-/-}$ mice, oxidative stress reduces the ability of primary melanoma cells to metastasize, whereas treatment with antioxidants enhanced metastasis (18).

We hypothesize that at least two mechanisms of relevance to melanoma metastasis and ROS-mediated oxidant stress are operable in immunocompetent mice, that is, direct effects of ROS on tumor cells that may either inhibit or enhance melanoma cell expansion, and oxidant-induced immunosuppression that may promote tumor growth and metastasis. The relative significance of these partly opposing mechanisms may relate to the sensitivity of melanoma cells to the growth-promoting or toxic effects of ROS as well as to the sensitivity of melanoma cells to immune-mediated clearance. This view may, at least in part, explain the contradiction that the *in vivo* administration of ROS-scavenging antioxidants such as *N*-acetylcysteine promotes as well as prevents murine melanoma metastasis (15–17).

The source of ROS may be critical for its capacity to promote or inhibit tumor progression. In our model, only ROS derived from NOX2-sufficient myeloid cells were targeted. In contrast, ROS scavengers such as *N*-acetyl-cysteine may also neutralize ROS generated from other sources, including those formed in mitochondria during cell respiration (16). The notion that NOX2^{+} myeloid cells may facilitate melanoma metastasis is supported by the findings that neutrophil infiltration of human primary melanomas heralds early metastatic spread (43) and that the exposure of murine cutaneous melanomas to UV light or chemical carcinogens triggers neutrophil-dependent inflammation that promotes metastasis (44, 45). Indeed, the adoptive transfer of CD11b^{+}Ly6G^{+} neutrophilic granulocytes enhances the formation of lung metastases after i.v. inoculation of murine carcinoma cells (46). The effect was secondary to granulocyte-induced inhibition of NK-cell function. Neutrophil secretion of IL1β and matrix metalloproteinases contributed to tumor cell extravasation but the detailed mechanism of NK-cell inhibition was not defined (46).

Although further studies are required to clarify the detailed impact of granulocytes and other NOX^{+} myeloid cells for the course of cancer, our results imply that the release of NOX2-derived ROS from these cells may constitute a mechanism of NK-cell inhibition during metastasis of relevance to these previous reports, and that strategies to target NOX2-derived ROS may facilitate NK cell–mediated clearance of metastatic cells. This assumption gains further support by the results of the present study showing that the depletion of Gr1^{+} cells reduced melanoma metastasis, and that NOX2 inhibition using HDC did not affect metastasis in Gr1^{+}-depleted animals. Additionally, the finding that IL15, an NK-cell–activating cytokine, improved the antimetastatic efficacy of pharmacologic NOX2 inhibition in WT animals suggests a combinatorial immunotherapy to reduce metastasis formation.

In summary, our results suggest that NOX2 function affects NK cell–mediated control of murine melanoma metastasis. We propose that pharmacologic inhibition of NOX2, alone or combined with immunostimulatory strategies, should be further evaluated in preventing melanoma metastasis.

Disclosure of Potential Conflicts of Interest

K. Hellstrand and A. Martner are authors of issued or pending patents protecting the use of histamine dihydrochloride in cancer immunotherapy. K. Hellstrand is a consultant/advisory board member for Consultancy Meda Pharma. No potential conflicts of interest were disclosed by the other authors.

Authors' Contributions

Conception and design: E. Aydin, K. Hellstrand, A. Martner
Development of methodology: E. Aydin, F.H. Nazir
Acquisition of data (provided animals, acquired and managed patients, provided facilities, etc.): E. Aydin, J. Johansson, F.H. Nazir
Analysis and interpretation of data (e.g., statistical analysis, biostatistics, computational analysis): E. Aydin, F.H. Nazir, K. Hellstrand
Writing, review, and/or revision of the manuscript: E. Aydin, J. Johansson, F.H. Nazir, K. Hellstrand, A. Martner
Administrative, technical, or material support (i.e., reporting or organizing data, constructing databases): E. Aydin
Study supervision: K. Hellstrand, A. Martner

Acknowledgments

We are grateful to Prof. Nils Lycke, MIVAC, University of Gothenburg, for providing the B6.129S7-*Ifng*^{tm1Ts}/J mice.

Grant Support

This work was supported by the Swedish Research Council (2012-2047 to A. Martner; 2012-3205 to K. Hellstrand), the Swedish Society for Medical Research (SSMF to A. Martner), the Swedish Cancer Society (CAN 212/595 to A. Martner; CAN 2015/411 to K. Hellstrand), the Swedish state via the ALF agreement (ALFGBG-436961 to A. Martner), the Erna and Victor Hasselblad Foundation (to A. Martner), the Torsten and Ragnar Söderberg Foundation (to K. Hellstrand), the Assar Gabrielsson Foundation (to E. Aydin), BioCARE—a National Strategic Research Program at University of Gothenburg and the Sahlgrenska Academy at University of Gothenburg (to A. Martner).

The costs of publication of this article were defrayed in part by the payment of page charges. This article must therefore be hereby marked *advertisement* in accordance with 18 U.S.C. Section 1734 solely to indicate this fact.

Received December 21, 2016; revised May 4, 2017; accepted July 20, 2017; published OnlineFirst July 31, 2017.

References

1. Karlsson A, Dahlgren C. Assembly and activation of the neutrophil NADPH oxidase in granule membranes. Antioxid Redox Signal 2002;4:49–60.
2. Geiszt M. NADPH oxidases: new kids on the block. Cardiovasc Res 2006; 71:289–99.
3. Kusmartsev S, Gabrilovich DI. Inhibition of myeloid cell differentiation in cancer: the role of reactive oxygen species. J Leukoc Biol 2003; 74:186–96.
4. Bedard K, Krause KH. The NOX family of ROS-generating NADPH oxidases: physiology and pathophysiology. Physiol Rev 2007;87:245–313.
5. Quinn MT, Gauss KA. Structure and regulation of the neutrophil respiratory burst oxidase: comparison with nonphagocyte oxidases. J Leukoc Biol 2004;76:760–81.
6. Hellstrand K, Asea A, Dahlgren C, Hermodsson S. Histaminergic regulation of NK cells. Role of monocyte-derived reactive oxygen metabolites. J Immunol 1994;153:4940–7.
7. Hansson M, Asea A, Ersson U, Hermodsson S, Hellstrand K. Induction of apoptosis in NK cells by monocyte-derived reactive oxygen metabolites. J Immunol 1996;156:42–7.

8. Kono K, Salazar-Onfray F, Petersson M, Hansson J, Masucci G, Wasserman K, et al. Hydrogen peroxide secreted by tumor-derived macrophages down-modulates signal-transducing zeta molecules and inhibits tumor-specific T cell-and natural killer cell-mediated cytotoxicity. Eur J Immunol 1996;26:1308–13.
9. Aurelius J, Martner A, Brune M, Palmqvist L, Hansson M, Hellstrand K, et al. Remission maintenance in acute myeloid leukemia: impact of functional histamine H2 receptors expressed by leukemic cells. Haematologica 2012;97:1904–8.
10. Kiessling R, Wasserman K, Horiguchi S, Kono K, Sjoberg J, Pisa P, et al. Tumor-induced immune dysfunction. Cancer Immunol Immunother 1999;48:353–62.
11. Hellstrand K, Brune M, Naredi P, Mellqvist UH, Hansson M, Gehlsen KR, et al. Histamine: a novel approach to cancer immunotherapy. Cancer Invest 2000;18:347–55.
12. Martner A, Thoren FB, Aurelius J, Hellstrand K. Immunotherapeutic strategies for relapse control in acute myeloid leukemia. Blood Rev 2013; 27:209–16.
13. Kelkka T, Pizzolla A, Laurila JP, Friman T, Gustafsson R, Kallberg E, et al. Mice lacking NCF1 exhibit reduced growth of implanted melanoma and carcinoma tumors. PLoS One 2013;8:e84148.
14. Ligtenberg MA, Cinar O, Holmdahl R, Mougiakakos D, Kiessling R. Methylcholanthrene-induced sarcomas develop independently from NOX2-Derived ROS. PLoS One 2015;10:e0129786.
15. De Flora S, D'Agostini F, Masiello L, Giunciuglio D, Albini A. Synergism between N-acetylcysteine and doxorubicin in the prevention of tumorigenicity and metastasis in murine models. Int J Cancer 1996;67:842–8.
16. Le Gal K, Ibrahim MX, Wiel C, Sayin VI, Akula MK, Karlsson C, et al. Antioxidants can increase melanoma metastasis in mice. Sci Transl Med 2015;7:308re8.
17. Sayin VI, Ibrahim MX, Larsson E, Nilsson JA, Lindahl P, Bergo MO. Antioxidants accelerate lung cancer progression in mice. Sci Transl Med 2014;6:221ra15.
18. Piskounova E, Agathocleous M, Murphy MM, Hu Z, Huddlestun SE, Zhao Z, et al. Oxidative stress inhibits distant metastasis by human melanoma cells. Nature 2015;527:186–91.
19. Dalton DK, Pitts-Meek S, Keshav S, Figari IS, Bradley A, Stewart TA. Multiple defects of immune cell function in mice with disrupted interferon-gamma genes. Science 1993;259:1739–42.
20. Dahlgren C, Karlsson A. Respiratory burst in human neutrophils. J Immunol Methods 1999;232:3–14.
21. Coffelt SB, Kersten K, Doornebal CW, Weiden J, Vrijland K, Hau CS, et al. IL-17-producing gammadelta T cells and neutrophils conspire to promote breast cancer metastasis. Nature 2015;522:345–8
22. Betten A, Dahlgren C, Hermodsson S, Hellstrand K. Histamine inhibits neutrophil NADPH oxidase activity triggered by the lipoxin A4 receptor-specific peptide agonist Trp-Lys-Tyr-Met-Val-Met. Scand J Immunol 2003;58:321–6.
23. Hellstrand K, Asea A, Hermodsson S. Role of histamine in natural killer cell-mediated resistance against tumor cells. J Immunol 1990;145:4365–70.
24. Fehniger TA, Caligiuri MA. Interleukin 15: biology and relevance to human disease. Blood 2001;97:14–32.
25. Fidler IJ, Nicolson GL. Organ selectivity for implantation survival and growth of B16 melanoma variant tumor lines. J Natl Cancer Inst 1976; 57:1199–202.
26. Corzo CA, Cotter MJ, Cheng P, Cheng F, Kusmartsev S, Sotomayor E, et al. Mechanism regulating reactive oxygen species in tumor-induced myeloid-derived suppressor cells. J Immunol 2009;182:5693–701.
27. Maghzal GJ, Krause KH, Stocker R, Jaquet V. Detection of reactive oxygen species derived from the family of NOX NADPH oxidases. Free Radic Biol Med 2012;53:1903–18.
28. Saijo N, Ozaki A, Beppu Y, Takahashi K, Fujita J, Sasaki Y, et al. Analysis of metastatic spread and growth of tumor cells in mice with depressed natural killer activity by anti-asialo GM1 antibody or anticancer agents. J Cancer Res Clin Oncol 1984;107:157–63.
29. Takeda K, Nakayama M, Sakaki M, Hayakawa Y, Imawari M, Ogasawara K, et al. IFN-gamma production by lung NK cells is critical for the natural resistance to pulmonary metastasis of B16 melanoma in mice. J Leukoc Biol 2011;90:777–85.
30. Kakuta S, Tagawa Y, Shibata S, Nanno M, Iwakura Y. Inhibition of B16 melanoma experimental metastasis by interferon-gamma through direct inhibition of cell proliferation and activation of antitumour host mechanisms. Immunology 2002;105:92–100.
31. Martner A, Wiktorin HG, Lenox B, Ewald Sander F, Aydin E, Aurelius J, et al. Histamine promotes the development of monocyte-derived dendritic cells and reduces tumor growth by targeting the myeloid NADPH oxidase. J Immunol 2015;194:5014–21.
32. Szatrowski TP, Nathan CF. Production of large amounts of hydrogen peroxide by human tumor cells. Cancer Res 1991;51:794–8.
33. Panieri E, Santoro MM. ROS homeostasis and metabolism: a dangerous liason in cancer cells. Cell Death Dis 2016;7:e2253.
34. Galadari S, Rahman A, Pallichankandy S, Thayyullathil F. Reactive oxygen species and cancer paradox: to promote or to suppress? Free Radic Biol Med 2017;104:144–64.
35. Nelson KK, Melendez JA. Mitochondrial redox control of matrix metalloproteinases. Free Radic Biol Med 2004;37:768–84.
36. Diaz B, Shani G, Pass I, Anderson D, Quintavalle M, Courtneidge SA. Tks5-dependent, nox-mediated generation of reactive oxygen species is necessary for invadopodia formation. Sci Signal 2009;2:ra53.
37. Diaz B, Courtneidge SA. Redox signaling at invasive microdomains in cancer cells. Free Radic Biol Med 2012;52:247–56.
38. Teoh-Fitzgerald ML, Fitzgerald MP, Zhong W, Askeland RW, Domann FE. Epigenetic reprogramming governs EcSOD expression during human mammary epithelial cell differentiation, tumorigenesis and metastasis. Oncogene 2014;33:358–68.
39. Schumacker PT. Reactive oxygen species in cancer: a dance with the devil. Cancer Cell 2015;27:156–7.
40. Nishikawa M. Reactive oxygen species in tumor metastasis. Cancer Lett 2008;266:53–9.
41. Lee JH, Won YS, Park KH, Lee MK, Tachibana H, Yamada K, et al. Celastrol inhibits growth and induces apoptotic cell death in melanoma cells via the activation ROS-dependent mitochondrial pathway and the suppression of PI3K/AKT signaling. Apoptosis 2012;17:1275–86.
42. Tsai MH, Liu JF, Chiang YC, Hu SC, Hsu LF, Lin YC, et al. Artocarpin, an isoprenyl flavonoid, induces p53-dependent or independent apoptosis via ROS-mediated MAPKs and Akt activation in non-small cell lung cancer cells. Oncotarget 2017; doi: 10.18632/oncotarget.16058
43. Jensen TO, Schmidt H, Moller HJ, Donskov F, Hoyer M, Sjoegren P, et al. Intratumoral neutrophils and plasmacytoid dendritic cells indicate poor prognosis and are associated with pSTAT3 expression in AJCC stage I/II melanoma. Cancer 2012;118:2476–85.
44. Bald T, Quast T, Landsberg J, Rogava M, Glodde N, Lopez-Ramos D, et al. Ultraviolet-radiation-induced inflammation promotes angiotropism and metastasis in melanoma. Nature 2014;507:109–13.
45. Bald T, Landsberg J, Jansen P, Gaffal E, Tuting T. Phorbol ester-induced neutrophilic inflammatory responses selectively promote metastatic spread of melanoma in a TLR4-dependent manner. Oncoimmunology 2016;5:e1078964.
46. Spiegel A, Brooks MW, Houshyar S, Reinhardt F, Ardolino M, Fessler E, et al. Neutrophils suppress intraluminal NK cell-mediated tumor cell clearance and enhance extravasation of disseminated carcinoma cells. Cancer Discov 2016;6:630–49.